STUDY OF ARRAY SOUNDFIELD CHARACTERISTICS UNDER CODED EXCITATION

S. H. Tretbar, D. Schmitt, C. Günther, M. Hoß, P. K. Weber and R. M. Lemor
Fraunhofer Institute for Biomedical Engineering IBMT, Ensheimer Strasse 48, 66386, St Ingbert, Germany
steffen.tretbar@ibmt.fraunhofer.de

Abstract

For navigation in lateral skull base interventions the exact measurement of the skull shape and thickness is a key issue. Single element ultrasonic methods using coded signals can determine those parameters with the desired accuracy. Like in other medical ultrasonic fields arrays promise more control on the soundfield and faster data acquisition. On the other hand a complex transmit signal influences the soundfield of an array driven by multi-channel electronics. This has to be considered implementing beamforming strategies for coded signals. A numerical model taking into account the excitation signal, the transducer and the beamformer settings is needed to optimise this system. Recent work was focused on the investigation of single element transducers under coded excitation. As a result our numerical method was validated with experimental findings. The soundfield calculation method used was extended to take into account linear array transducers with electronic beamsteering. The influence of different codes like modified bursts, chirps and Barker codes have been simulated under special beamformer settings. The position and the shape of the focal zone was studied since this is a crucial parameter for the target application of skull thickness estimation. Several signals are implemented in a multichannel digital beamformer hardware. Measurements of linear array transducers with a sound field hydrophone scanner are presented.

Introduction

Navigation and registration based on X-ray and MR imaging is well established in many medical interventions. Ultrasound based methods offer non-invasive, real-time and cost-effective alternatives. A challenging field is milling of the lateral skull base for cochlear implants as reported by Plinkert et al. [1]. High frequencies are needed to ensure the demanded accuracy of 0.5 mm in bone (c = 2600 m/s). The high acoustic damping in skull bone (2,86 dB/mm*MHz) is limiting the frequency to 0.5 – 1 MHz. Pulse compression based on coded signals shall be used to increase energy entry and spatial resolution. Matched filters shall be used as reported in literature [2-8]. Selection of the appropriate code for the target application is a key issue.

The goal of the work presented here was studying the influence of different pulses on the performance of a cross-correlation based thickness measurement of bony structures with linear phased array transducers. Different codes have been selected and the potential axial resolution has been studied deriving figures of merit based on an auto-correlation approach. The codes are implemented into a PC-based DiPhAS-Beamformer hardware.

For a high-bandwidth linear phased array probe the resulting sound-fields are measured in a fully automated hydrophone 3D scanner system. The sound-fields have been simulated based on a point-source-synthesis approach. Focus dimensions of the sound-fields are evaluated as a figure of merit. A linear chirp has been chosen as the optimum for the target application.

Methods

Coded signals and signal processing

Besides three generic signals, a pseudo pulse (20MHz-burst), a single burst (Burst1) and a three cycles burst (Burst3), a pseudo-random binary signals (Barker5) as well as a linear frequency-modulated pulse (Chirp3-9) have been studied. Pseudo-random binary signals can be described as

$$x_{\mathrm{mod}}(t) = \sum_{n=1}^{N} a_n \Pi_n(t) \exp[i(\varpi_0 t + \varphi_0)] \quad (1)$$

with a_n being the amplitude of n-th binary element, τ the duration, φ_n the phase angle, N the number of the elements and

$$\Pi_n(t) = \begin{cases} 1 \rightarrow \text{if } (n-1)\tau \le t \le n\tau \\ 0 \rightarrow \text{else.} \end{cases} \quad (2)$$

Three different codings are possible

1. $a_n = 1$ and $\varphi_n = 0$ or π
2. $a_n = 1$ and φ_n variable
3. a_n and φ_n variable,

the code chosen (Barker5) belonging to the first group.

The representation of a linear frequency-modulated pulse can be written as

$$x(t) = rect\left(\frac{2t - T}{T}\right) \cdot \cos(2\pi(f_1 t + \frac{1}{2} k t^2)) \quad (3)$$

with $$k = \frac{f_2 - f_1}{T}, \quad (4)$$

f_1 and f_2 representing start and stop frequency and T being the duration of the pulse.
The signals are chosen to have an auto-correlation function similar to a Dirac pulse [[7]]. In this case the impulse response of the system corresponds to the cross-correlation between transmit and receive signal. The auto-correlation enables estimation of the axial resolution based on the main-side-lobe relation. The lower the main-side-lobe relation the better is the axial resolution for a distance or thickness measurement.
Depending on the transmit frequency an amplitude gain (AG) can be defined to describe the gain in signal to noise ratio. This defines a second important figure of merit [6,8]. The amplitude gain is defined as the square root of the product of signal bandwidth *B* and length *T* [8]:

$$AG = \sqrt{B * T} \qquad (5)$$

Sound-field simulation and parameters

Basically in a homogeneous fluid the calculation of the sound-field is equivalent to solving for the wave equation under given boundary conditions. For the pressure p at a location $\vec{r}$ and a time t the wave equation in a fluid writes

$$\frac{\partial^2}{\partial t^2} p(\vec{r},t) - \frac{1}{\kappa} div\left\{\frac{1}{\rho} grad\left[p(\vec{r},t)\right]\right\} = 0 \qquad (6)$$

with fluid density ρ and compressibility κ. The implemented approach for the calculation of the sound-field is according to Huygen's principle. The radiating surface of the transducer (aperture) is covered with point sources. Each of them transmits a spherical wave into the half space in front of the transducer. At any point the total pressure can be calculated superimposing the contribution of all sources. To get the one way radiation pattern the normalized pressure distribution is calculated to the maximum pressure (usually in the focal point) [9].
The code implemented to simulate the sound-field performance supports all types of transducers (single element, linear- and 2D-arrays) and driving signals. In our case experimentally derived pressure signals in the focus are used to drive the virtual transducer. All types of focusing and beam-steering strategies can be studied.
Figure 1 shows the derived sound-field in a plane in front of the transducer. The markers show the –3 dB width (lateral) and length (axial) of the focus defined as figures of merit for the sound-field. The smaller those values the more concentrated is the pressure distribution increasing the intensity at the point of interest.

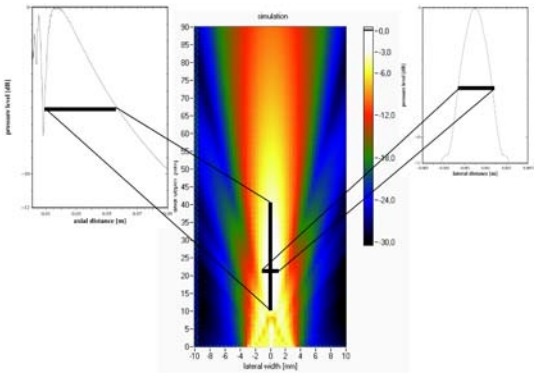

Figure 1:Sound-field with marked –3 dB dimension Of the focus in lateral and axial direction.

Experimental setup

The sound-field of 64 elements of a 144 element linear phased array transducer probe with 3-11MHz bandwidth is measured for the different signals. The mechanical part of the system is a motorized 3D scanner system with a range of 500 x 500 x 500 mm^3. Minimum step width is 0.1 mm with a position accuracy of 0.01 mm. The beamformer electronic is a 64 channel **Di**gital **Ph**ased **A**rray **S**ystem (DiPhAS) developed at Fraunhofer IBMT. It is PC-based and fully programmable for each channel. Frequency range is 0.5 – 10 MHz with transmit voltage 160V_{pp} (200 Ω). Receive gain is up to 72 dB with a bandwidth of 20 MHz. Analog/digital conversion is done by a 12 bit ADC. Transmit signal is free programmable. The high speed rf-data acquisition is a 40MHz/16bit IO card through PCI-bus data processing in PC. Bursts, linear and non-linear chirps, Barker and Golay codes are accessible via a signal generator panel. A 0.4 mm aperture hydrophone (1 – 20 MHz) with 50 nV/Pa sensitivity is used for reception. An axial plane of 30 x 60 mm^2 was extracted from a 3D scanned soundfield for all transducer/signal combinations with a step-width of 0.5 mm.

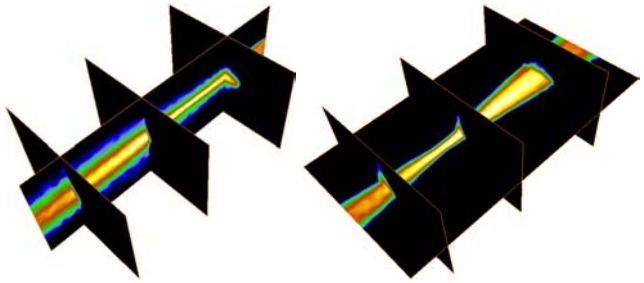

Figure 2: Measured 3D Sound-field

Results

The next figures give the measured and simulated sound-field in a plane in front of the phased linear array in space direction (64 elements, pitch 265µm). The color coded value represents the sound peak-peak-pressure relative to the focal pressure in dB. The transducer was electronically focused on z-axis to 40 mm. On reception dynamic focusing was applied. For the simulation, the same strategy was applied. The excitation signals were chosen with respect to the bandwidth limits of the transducer. For the single frequency burst signals the frequency was chosen to provide highest pressure in the focus (3.76 MHz). The pseudo-pulse was generated using the shortest electrical switching supported by the electronics (20 MHz). The derived figures of merit are summarized in tab. 1.

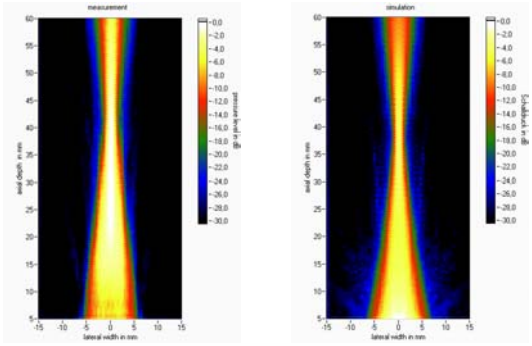

Figure 3a

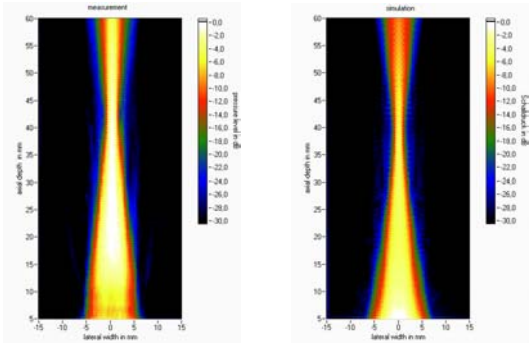

Figure 3b

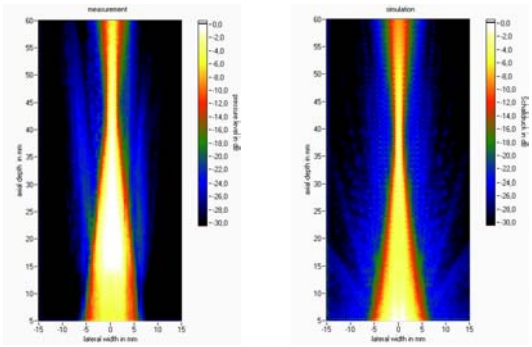

Figure 3c

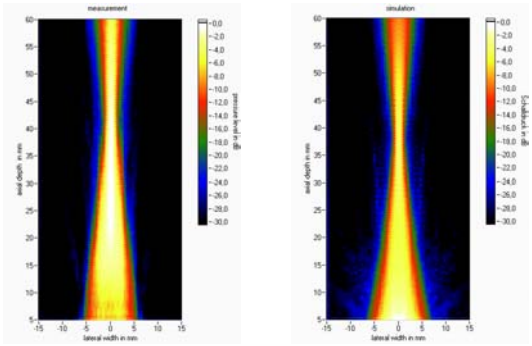

Figure 3d

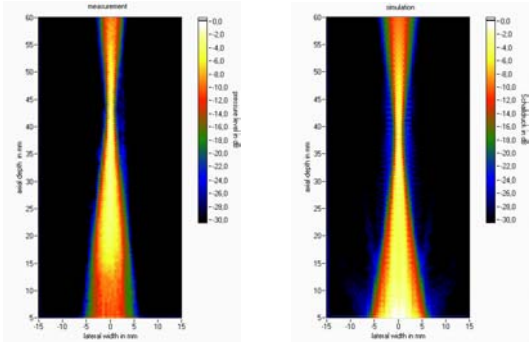

Figure 3e

Figure 3 (a) burst 1 (3,76 MHz), (b) burst 3 (3,76 MHz), (c) linear Chirp 3-9MHz, (d) Barker 5 and (e) Pseudo Pulse (Burst1 20 MHz) with measured and simulated sound-field

Table I: Summary of the derived figures of merit.

Frequency [MHz]	Burst1 3.76	Burst3 3.76	Chirp 3-9	Barker 5	Pulse
main-side-lobe relation	0.35	0.78	0.19	0.57	0.19
amplitude gain	1.3	1.45	2.57	2.1	1.63
6 dB bandwidth [MHz]	1.7	1.2	5.5	2.0	5.3
max. pressure Ppp [MPa]	4.250	5.10	5.27	4.83	3.01
focus depth [mm]	40	40	40	40	40
focus length/width [mm]	45/4	42/5	41/4	38/4	32/0.5

Discussion

As given in table I the chirp signal scores best on the main-side-lobe relation and in amplitude gain.
This promises best results for the measurement of the skull thickness based on pulse-compression technique. The main-side-lobe relation on pseudo pulse signal has the same value as the chirp signal but the amplitude gain and the maximum peak-peak pressure are much lower. This results in an unsufficient energy entry in the high damping human skull bone. The

Barker code has a good main-side-lobe relation, bandwidth and amplitude gain. This makes the Barker signal a good choice if a short signal is necessary for coded excitation. The single frequency signal Burst3 delivers high energy in the focal point but the high main-side-lobe relation limits the axial resolution.
The electronically controlled focus depth is found to be independent from the excitation signal.
Based on the figures of merit defined the Chirp signal is the best candidate for the thickness measurement of the skull.

Conclusion

For the measurement of the human skull bone thickness an ultrasonic cross-correlation technique based on coded signals is proposed. Different codes were implemented into the DiPhAS beamformer hardware and measured with a new 3D sound field scanning and visualization system.
The influence of coded signals on the sound field of an electronically focused high-bandwidth linear array probe was simulated, measured and evaluated.
A point source synthesis method enabled parallel calculation of the sound-field. Figures of merit for a comparison of the codes are introduced. Main-side-lobe relation and amplitude gain are derived from the auto-correlation of the acoustical pulse. Focal zone dimensions are used to characterize the sound field.
In contrast to the previously reported shift in the natural focus of single element transducers an adaptation of focusing delay for different codes is not necessary. The relation between axial resolution with correlation techniques and chosen code follows the same rules for single element transducers and focused arrays. So the coded excitation technique for arrays can take full advantage of electronic possibilities (adaptive focusing, beam steering and fast scanning).
The chirp promises the best results for skull base registration.

Acknowledgement

The authors would like to thank Prof. Plinkert and his team at Saarland University in Homburg, Germany for the support.

References

[1] P.K. Plinkert, B. Plinkert, A. Hiller, J. Stallkamp „Einsatz eines Roboters an der lateralen Schädelbasis“ HNO Vol. 49, Springer-Verlag, 2001.
[2] C. R. Meyer „An Iterative, Parametric Spectral Estimation Technique for High-Resolution Puls-Echo Ultrasound“, IEEE Trans. on Biomedical Engineering, Vol. BME-26, NO. 4, April 1979.
[3] M. O`Donnell „Coded Ecxitation System for Improving the Penetration of Real-Time Phased-Array Imaging System“, IEEE Trans. on Ultras., Ferroel., and Freq. Control, Vol. 39, NO. 3, 1992.
[4] P.-C. Li, E. Ebbini, M. O`Donnell „A New Filter Design Technique for Coded Ecxitation System“, IEEE Trans. on Ultras., Ferroel., and Freq. Control, Vol. 39, NO. 6, 1992.
[5] T. Folkestad, K. S. Mylvaganam „Chirp Ecxitation of Ultrasound Probes and Algorithm for Filtering Transit Times in High-Rangeability Gas Flow Metering“, IEEE Trans. on Ultras., Ferroel., and Freq. Control, Vol. 40, NO. 3, 1993.
[6] M. Pollakowski „Ein Beitrag zur Anwendung der Pulskompressionstechnik in der zerstörungsfreien Werkstoffprüfung mit Ultraschall“, Aachen: Shaker Verlag, 1993
[7] M. A. Benkhelifa, M. Gindre, J.-Y. le Huerou, W. Urbach „Echography Using Correlation Techniques: Choice of Coded Signal“, IEEE Trans. on Ultras., Ferroel., and Freq. Control, Vol. 41, NO. 5, 1994.
[8] M. Pollakowski, H. Ermert „Chirp Signal Matching and Signal Power Optimization in Pulse-Echo Mode”, Ultrasonic Nondestructive Testing IEEE Trans. on Ultras., Ferroel., and Freq. Control, Vol. 41, NO. 5, 1994.
[9] B.D. Steinberg “Principles of Aperture and Array System Design” Wiley & Sons, New York, 1976.
[10] Steffen H. Tretbar and Daniel Schmitt „Coded Signals for Intraoperative Registration of the Human Skull”, Proceedings 27th Acoustical Imaging, Saarbrücken, Germany 2003 (in press)